International Journal of Engineering Research & Technology (IJERT)
ISSN: 2278-0181
Vol. 15 Issue 02 , February - 2026

Hybrid Fuel - Solar Powered Bidirectional Charging System for Electric Vehicles

Dr. V. Senthil Nayagam, Steve Ishan. Y, Daniel. J
Department Of Electrical And Electronics Engineering
Sathyabama Institute Of Science And Technology, Chennai, India

Abstract: This study focuses on the development of an effective closed-loop control scheme for a bidirectional DC–DC converter employing a phase-shift controlled, high-frequency full-bridge resonant architecture. The converter's performance is analyzed under two different control approaches, namely proportional–integral–derivative (PID) control and sliding mode control (SMC). The transient and steady-state characteristics of the system are comparatively evaluated in terms of rise time, peak overshoot, settling duration, and steady-state regulation accuracy. A small-signal representation of the converter is derived to support controller synthesis and stability evaluation. The proposed converter topology and control methodologies are validated through MATLAB/Simulink-based simulations and experimental testing across multiple operating scenarios.

Keywords: Bidirectional DC–DC converter, Phase-shift modulation, Sliding mode control, PID controller, Electric vehicle charging.

1. INTRODUCTION

The rapid growth of electric vehicles (EVs) has intensified the demand for efficient, reliable, and flexible power conversion systems capable of supporting diverse energy sources and operating conditions. To address challenges related to energy efficiency, charging speed, and grid interaction, bidirectional DC–DC converters have emerged as a key enabling technology in modern EV charging and energy management systems. These converters allow controlled power flow between batteries, renewable energy sources, and the utility grid, thereby supporting advanced functionalities such as vehicle-to-grid (V2G), grid-to-vehicle (G2V), and hybrid energy storage integration [1], [6].

Recent research has focused extensively on improving converter topologies to achieve high efficiency, reduced switching losses, and enhanced power density. Isolated and non-isolated bidirectional DC–DC converter structures, including resonant, multilevel, and high-gain configurations, have been proposed for EV and renewable energy applications [1], [9], [12]. Resonant and soft-switching techniques are particularly attractive due to their ability to minimize switching stress and electromagnetic interference while enabling high-frequency operation [10], [17]. Such characteristics are essential for compact onboard chargers and fast-charging infrastructure.

In addition to hardware advancements, control strategy plays a crucial role in determining the dynamic and steady-state performance of bidirectional converters. Conventional proportional–integral–derivative (PID) controllers remain widely adopted due to their simplicity and ease of implementation; however, their performance may degrade under parameter variations, nonlinear operating regions, and rapid load changes [15], [19]. To overcome these limitations, advanced nonlinear control techniques, especially sliding mode control (SMC), have gained significant attention. SMC offers strong robustness against disturbances and uncertainties, making it well suited for EV charging systems operating under fluctuating source and load conditions [2], [5], [14].

Several recent studies have demonstrated that SMC-based bidirectional converters exhibit superior transient response, reduced steady-state error, and improved stability compared to traditional linear controllers [2], [13], [20]. Furthermore, hybrid control approaches combining SMC with adaptive or intelligent methods have been proposed to enhance system robustness while mitigating chattering effects [3], [11]. Accurate small-signal modeling has also been emphasized as a vital step in controller design and stability analysis, enabling systematic comparison between different control strategies [4], [16].

The integration of renewable energy sources such as solar photovoltaic (PV) systems with EV charging infrastructure has further increased the complexity of power conversion and control. Bidirectional DC–DC converters facilitate efficient energy exchange between PV sources, battery storage, and the EV powertrain, thereby improving system flexibility and sustainability [4], [7], [8]. Recent works highlight the importance of coordinated control schemes that ensure stable operation under varying irradiation, battery state-of-charge, and grid conditions [6], [11], [18].

Motivated by these developments, this paper investigates a closed-loop bidirectional DC–DC converter based on a phase-shift modulated high-frequency full-bridge resonant topology for hybrid EV charging applications. The dynamic performance of conventional PID control is systematically compared with sliding mode control in terms of rise time, overshoot, settling time, and steady-state error. A small-signal model is developed to support controller design and stability evaluation. The effectiveness of the proposed approach is validated through MATLAB/Simulink

International Journal of Engineering Research & Technology (IJERT)
ISSN: 2278-0181
Vol. 15 Issue 02 , February - 2026

simulations and experimental results under different operating modes.

2. SYSTEM DESCRIPTION

Fig. 1 illustrates the overall architecture of the proposed hybrid fuel–solar powered bidirectional charging system intended for electric vehicle applications. The photovoltaic (PV) source serves as the primary energy input and is interfaced with Converter-1, which performs initial DC voltage regulation. This converter is operated using a pulse-width modulation (PWM) strategy to control the power extracted from the PV source.

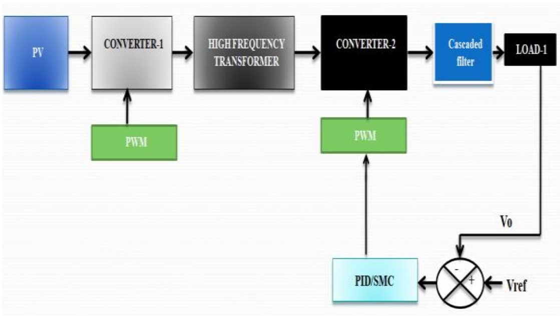

Fig-1: Closed loop simulation block diagram of onboard charging DC-DC converter with PID/SM controlled system

The regulated DC output is supplied to a high-frequency transformer, which provides galvanic isolation between the source and load while enabling voltage matching through high-frequency operation. On the secondary side, Converter-2 is employed as a bidirectional DC–DC converter, allowing controlled power transfer in both forward and reverse directions, thereby supporting battery charging and discharging modes.

A cascaded output filter is connected at the converter output to attenuate high-frequency switching ripples and improve the quality of the DC output voltage. The filtered output is delivered to the load, representing the EV battery or DC bus. The output voltage Vo is sensed and compared with the reference voltage Vref. The resulting error signal is processed by a hybrid PID–Sliding Mode Controller (PID-SMC), which generates appropriate PWM signals for Converter-2. This control approach ensures accurate voltage regulation, fast dynamic response, and enhanced robustness against source and load disturbances.

2.1.PID controller

A proportional–integral–derivative controller (PID controller or three-term controller) is a control loop mechanism employing feedback that is widely used in industrial control systems and a variety of other applications requiring continuously modulated control. A PID controller continuously calculates an error value.

The basic idea behind a PID controller is to read a sensor, then compute the desired actuator output by calculating proportional, integral, and derivative responses and summing those three components to compute the output.

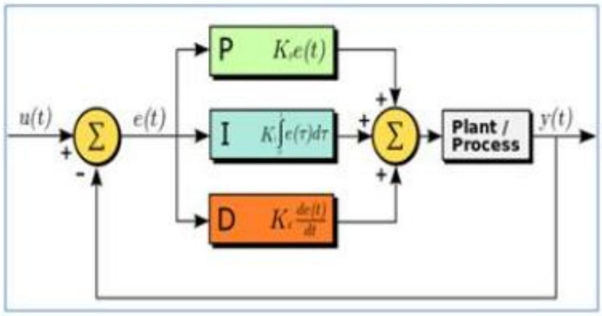

Fig-2: Block diagram of PID controller

2.2. Sliding Mode Controller

The block--diagram of 'SMC' is appeared in Fig-3. In SM, the preponderance of the controller comprise error of single or copious states of the-system in the sliding-surface.

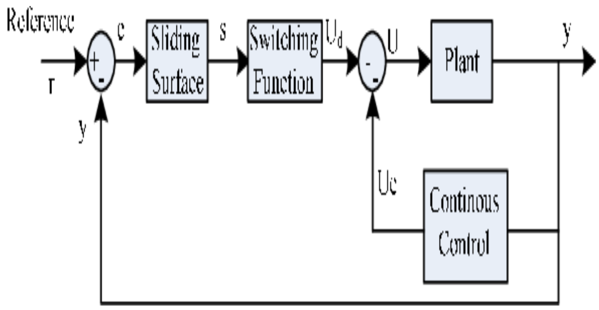

Fig-3: Block-Diagram of Slide Mode Controller.

Furthermore, a few-controller comprise error &both of the time-derivatives and the -integral of the-error in the sliding-surface to stabilize the-system. In this-case, the sliding-surface can be symbolized as a 2^{nd}-order deferential equation-for which broad numerical study is obliged to guarantee-system-steadiness. Another surface is characterized in for the enhancement in the steady-state-error& settling-time, which comprises voltage-error &square of the capacitor-current.

3. PROPOSED METHODOLOGY

A. Operating Principle of the Bidirectional Resonant Converter

The proposed system employs a phase-shift modulated full-bridge resonant DC–DC converter to enable bidirectional power transfer between the renewable source and the electric vehicle battery. The converter operates in two modes depending on the direction of power flow:

International Journal of Engineering Research & Technology (IJERT)
ISSN: 2278-0181
Vol. 15 Issue 02 , February - 2026

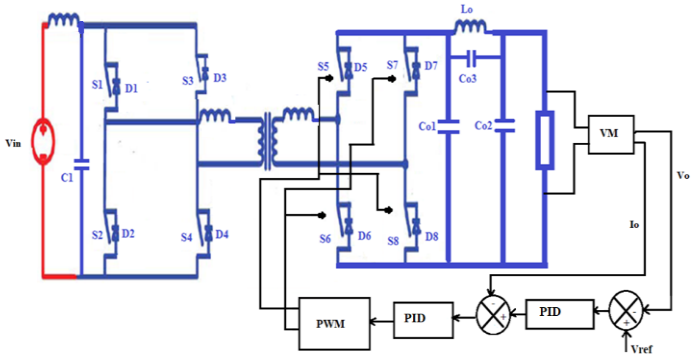

Fig-4: Closed Loop Circuit Diagram Of Bi-Directional DC-DC Converter With PID Controlled System

The Proposed Circuit Diagram of closed loop PID/SM controlled Bi-Directional DC-DC Converter with Cascaded-Filter system is shown in fig 2.4 and fig 2.5.

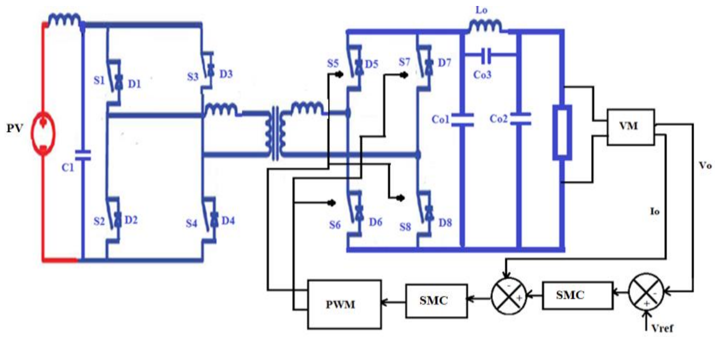

Fig-5: Closed Loop Circuit Diagram Of Bi-Directional DC-DC Converter With SM Controlled System

1. Forward Mode (Charging Mode):

Power flows from the PV source to the load. The primary-side full bridge switches S_1-S_4operate as an inverter, generating a high-frequency AC voltage that is transferred through the resonant tank and transformer. The secondary-side bridge S_5-S_8 functions as an active rectifier to regulate the DC output voltage.

2. Reverse Mode (Discharging Mode):

Power flows from the battery/load back to the source. The secondary bridge operates as an inverter, while the primary bridge performs rectification. The bidirectional nature of the switches enables seamless mode transition without additional hardware. Due to phase-shift control, the converter achieves zero-voltage switching (ZVS) for the power switches, resulting in reduced switching losses and improved efficiency.

B. Switching States and Phase-Shift Modulation

The full-bridge converter operates using phase-shift modulation between the two bridge legs. The effective duty cycle and transferred power are controlled by the phase difference ϕ between the gate signals.

- When switches S_1 and S_4 are ON, a positive voltage is applied across the transformer primary.
- When switches S_2 and S_3 are ON, a negative voltage is applied.
- The overlap period between switching states determines the energy transferred through the resonant tank.

By varying the phase shift angle ϕ, the output voltage and power flow direction are controlled without altering the switching frequency, which simplifies control and maintains soft-switching conditions.

C. Mathematical Model of the PID Controller

The error between the reference voltage and output voltage is expressed as

$$e(t)=V_{ref}-V_o$$

The PID controller output is given by

$$u_{PID}(t) = K_p e(t) + K_i \int_0^t e(\tau)\, d\tau + K_d \frac{de(t)}{dt}$$

where K_p, K_i, and K_d represent the proportional, integral, and derivative gains, respectively. The integral term eliminates steady-state error, while the proportional and derivative terms improve dynamic response.

D. Sliding Mode Control (SMC) Design

To enhance robustness against parameter variations and load disturbances, Sliding Mode Control is integrated with the PID controller. The sliding surface is defined as

$$s(t) = \lambda e(t) + \frac{de(t)}{dt}$$

where λ is a positive constant that determines the convergence speed.

The SMC control law is expressed as

$$u_{SMC}(t) = -K_s \operatorname{sign}(s(t))$$

where K_s is the sliding gain. This term forces the system states to converge rapidly toward the sliding surface, ensuring stable operation under uncertainties.

4. Results and Discussion of resonant DC-DC converter.

International Journal of Engineering Research & Technology (IJERT)
ISSN: 2278-0181
Vol. 15 Issue 02 , February - 2026

4.1 Open loop Proposed Bi-Directional DC-DC converter with cascaded filter for source Disturbance system

. Simulation parameters are presented in table1.

Table-1

Simulation parameters of modified LLC Resonant Converter

Vin	**20V**
L_2, L_3	**0.005µH**
L_1	**0.06µH**
C_3	**0.2µF**
C_1,C_2	**4200 µF**
C_2	**1500 µF**
R	**0.001 Ω**
R_{load}	**10 Ω**
Mosfet	**IRF840**
Diode	**IN4007**
Vo	**38V**

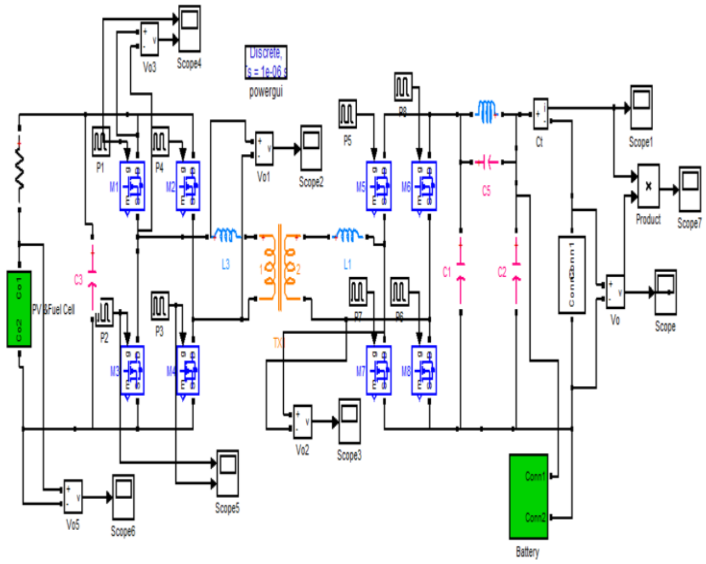

Fig-6: Proposed bidirectional DC-DC converter with soruce Disturbance

Fig. 6 shows the open-loop configuration of the bidirectional DC–DC converter with source disturbance. The input source is interfaced with a full-bridge converter, followed by a high-frequency transformer that provides electrical isolation and voltage matching. An LC output filter is used to reduce switching ripple, and measurement blocks are included to observe voltage, current, and power characteristics. This configuration is used to study the converter performance in open-loop operation. The input voltage waveform corresponding to this condition is presented in Fig. 7, with an input voltage of 18V.

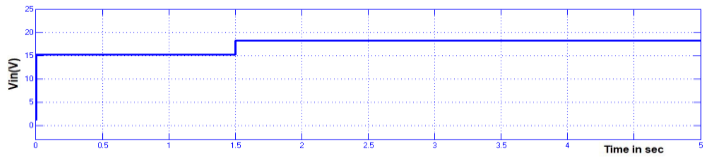

Fig-7: Input voltage across PV

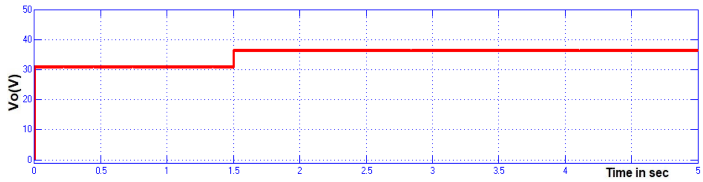

Fig-8: Voltage across battery Load

Fig. 8 illustrates the output voltage across the battery load of the bidirectional DC–DC converter under source disturbance conditions, with a measured value of 38 V. The corresponding output current delivered to the battery load is shown in Fig. 9 and is observed to be 2.5 A. Fig. 10 presents the output power of the bidirectional DC–DC converter under the same operating condition, which is approximately 87W.

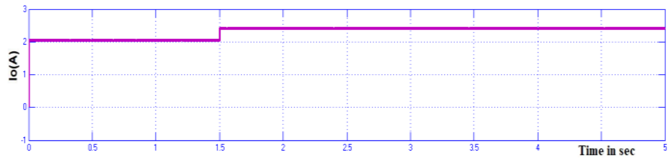

Fig-9: Current through battery- load

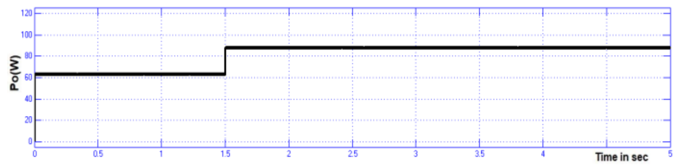

Fig-10: Output power

4.2 Closed loop Proposed Bi-Directional DC-DC converter with cascaded filter for PID controlled system

International Journal of Engineering Research & Technology (IJERT)
ISSN: 2278-0181
Vol. 15 Issue 02 , February - 2026

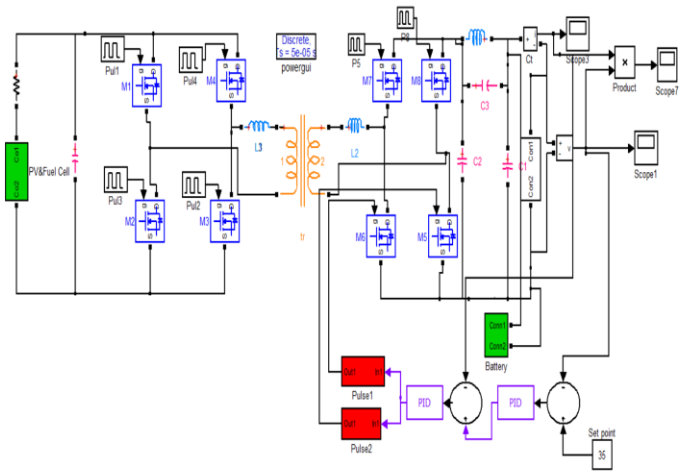

Fig-11: Proposed bidirectional DC-DC converter with PID controller

Fig-11 presents the circuit schematic of the proposed bidirectional DC–DC converter operating under a closed-loop PID-controlled scheme. The output voltage and current are sensed and compared with reference values, and the resulting error signals are processed by PID controllers. The controller outputs are used to generate PWM signals for the power switches, ensuring regulated output and improved dynamic performance under varying operating conditions. The corresponding input voltage waveform is illustrated in Fig-12, where the input voltage is maintained at 18 V.

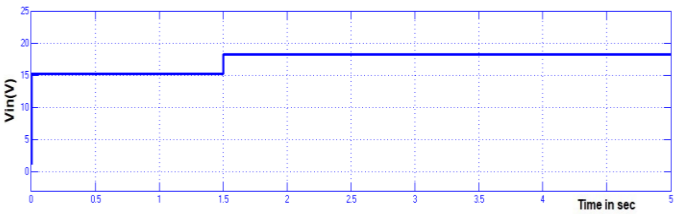

Fig-12: Input voltage across battery

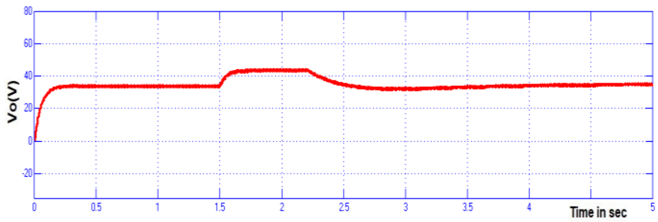

Fig-13: Voltage across battery Load

The output voltage across the battery load of the proposed bidirectional DC–DC converter with closed-loop PID control is depicted in Fig-13 and is maintained at 38 V. Fig-14 shows the output current flowing through the battery load, which reaches 2.8 A. The resulting output power of the converter is illustrated in Fig-15 and is measured to be 100 W.

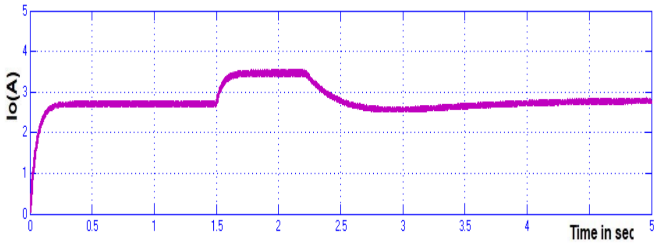

Fig-14: Current through battery- load

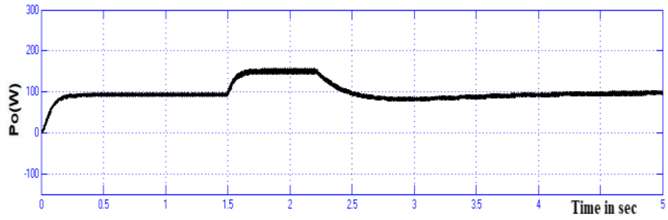

Fig-15: Output power

4.3 Closed loop Proposed Bi-Directional DC-DC converter with cascaded filter for Sliding Mode controlled system

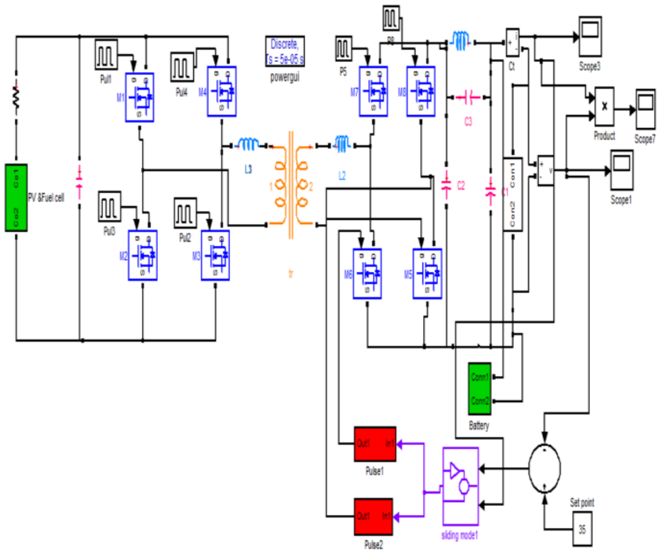

Fig-16: Proposed bidirectional DC-DC converter with sliding mode controller

The circuit configuration of the proposed bidirectional DC–DC converter employing closed-loop sliding mode control is shown in Fig-16. Fig-17depicts the input voltage applied to the converter, which is set to 18 V.

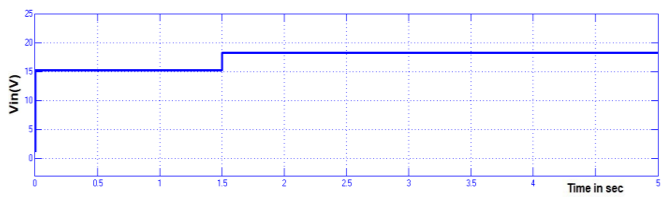

Fig-17: Input voltage

International Journal of Engineering Research & Technology (IJERT)
ISSN: 2278-0181
Vol. 15 Issue 02 , February - 2026

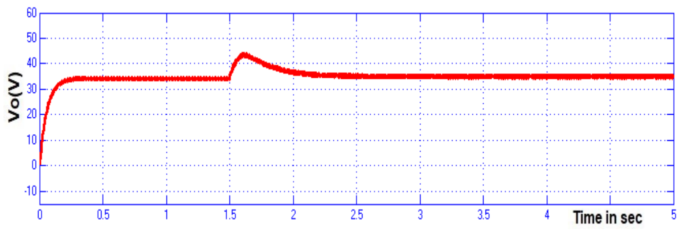

Fig-18: Voltage across battery Load

Fig-18 shows the output voltage across the battery load under closed-loop sliding mode control at 35 V. The corresponding output current is presented in Fig-19 with a magnitude of 2.8 A, while the output power of the proposed converter is illustrated in Fig-20 and is observed to be 100 W.

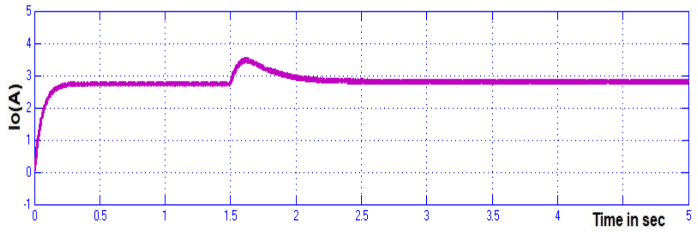

Fig-19: Current through battery- load

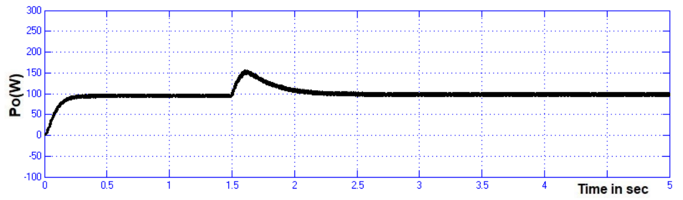

Fig-20: Output power

Table -2

Comparison of time domain parameters of voltage

Types of controller	Tr	Tp	Ts	Ess
PID	1.60	2.00	3.50	1.50
SMC	1.55	1.65	2.00	0.92

Table-2 summarizes the comparison of voltage time-domain performance parameters for the proposed closed-loop bidirectional DC–DC converter employing PID and sliding mode control strategies. The corresponding bar-chart representation of these parameters is illustrated in Fig-21.

It is observed that the implementation of the sliding mode controller based on the voltage reference significantly improves the dynamic response of the system. Specifically, the rise time is reduced from 1.6 s to 1.55 s, the peak time decreases from 2 s to 1.65 s, and the settling time is shortened from 3.5 s to 2 s. In addition, the steady-state voltage error is reduced from 1.5 V to 0.92 V when compared to the PID-controlled system.

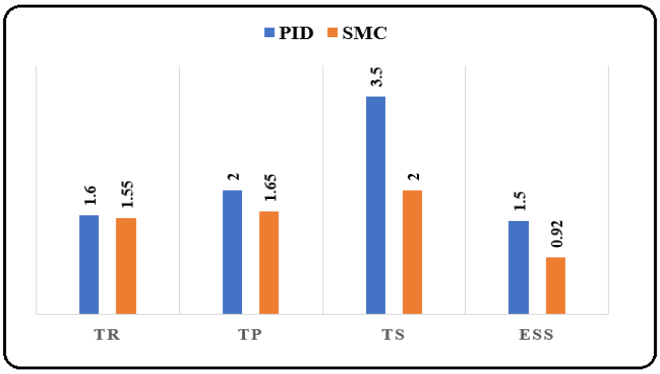

Fig-21:Bar chart Comparison of time domain parameters of voltage

Table -3

Comparison of time domain parameters of current

Types of controller	Tr	Tp	Ts	Ess
PID	1.59	1.98	3.50	0.3
SMC	1.55	1.64	2.00	0.1

Table-3 provides a comparative analysis of the current time-domain response characteristics of the proposed closed-loop bidirectional DC–DC converter using PID and sliding mode control approaches. The graphical comparison of these current performance indices is shown in Fig-22 in the form of a bar chart.

The analysis indicates that the sliding mode controller referenced to current control yields improved transient and steady-state behavior. In particular, the rise time decreases from 1.59 s to 1.55 s, while the peak time is reduced from 1.98 s to 1.64 s. Additionally, the settling time is shortened from 3.5 s to 2 s. A notable improvement is also observed in steady-state accuracy, with the current error reduced from 0.3 A to 0.1 A when compared to the PID-controlled system.

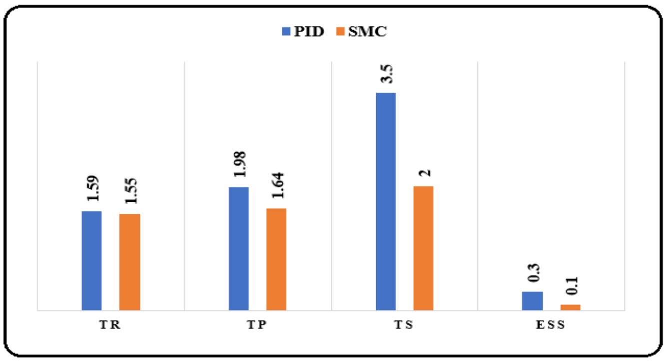

Fig-22: Bar chart Comparison of time domain parameters of current

5. CONCLUSION

The proposed bidirectional DC–DC converter is simulated under three operating conditions: with source disturbance, with a closed-loop PID controller, and with a closed-loop sliding mode controller (SMC). The simulation results are used to evaluate and compare the dynamic and steady-state performance of the control strategies. When the proposed converter operates under closed-loop sliding mode control with a voltage reference, a noticeable improvement in transient response is observed in comparison with the PID-controlled system. Specifically, the rise time is reduced from 1.60 s to 1.55 s, the peak time decreases from 2.00 s to 1.65 s, and the settling time is shortened from 3.50 s to 2.00 s. In addition, the steady-state voltage error is significantly reduced from 1.50 V to 0.92 V. Similarly, under current reference control, the sliding mode controller demonstrates superior performance. The rise time improves from 1.59 s to 1.55 s, the peak time decreases from 1.98 s to 1.64 s, and the settling time is reduced from 3.50 s to 2.00 s. Furthermore, the steady-state current error is minimized from 0.3 A to 0.1 A when compared to the PID-controlled case. Overall, the simulation outcomes confirm that the proposed closed-loop bidirectional DC–DC converter employing sliding mode control exhibits enhanced dynamic response, improved steady-state accuracy, and greater robustness against disturbances. These results clearly indicate that the sliding mode controller outperforms the conventional PID controller for bidirectional DC–DC converter applications.

REFERENCES

[1] A. Tuluhong et al., "Recent developments in bidirectional DC–DC converter topologies, control strategies, and applications in photovoltaic power generation systems: A comparative review and analysis," *Electronics*, 2025.

[2] U. G. Reddy et al., "Performance analysis of a high-gain bidirectional DC–DC converter fed EV drive with sliding mode controller for reduced ripple distortion," *Utilitas Mathematica*, 2024.

[3] M. R. Khan et al., "Accurate and optimal control of a bidirectional DC–DC converter using a robust adaptive approach," *Prime – Advances in Electrical Engineering, Electronics and Energy*, 2025.

[4] M. R. Khan et al., "Adaptive bidirectional DC–DC converter for solar PV-enabled electric vehicle charging systems," *Journal of Electrical Systems*, 2024.

[5] H. Wang et al., "Multivariable-feedback sliding-mode control of bidirectional DC–DC converter in DC microgrid for improved stability," *Electronics*, 2023.

[6] S. K. Singh et al., "A thorough review of energy management and advanced control techniques for bidirectional DC–DC converters in electric vehicle applications," *Results in Engineering*, 2025.

[7] I. Ahmed et al., "A bidirectional PV-grid connected electric vehicle framework for vehicle-to-grid and grid-to-vehicle applications," *COMPEL – The International Journal for Computation and Mathematics in Electrical and Electronic Engineering*, 2024.

[8] A. Pratama et al., "Design of bidirectional DC–DC converter for photovoltaic charging systems," *VUBETA Journal*, 2024.

[9] R. Kumar et al., "Bi-directional DC–DC converter for enhanced power management in electric vehicle applications," *IEEE Access*, 2025.

[10] A. Sakhare, "Advanced DC–DC converter topologies for electric vehicles," *IET Electric Power Applications*, 2025.

[11] K. Dhineshkumar et al., "Integrated MPPT and bidirectional DC–DC converter with intelligent control for renewable energy systems," *Scientific Reports*, 2025.

[12] M. Lingamaiah et al., "A vehicle-to-grid enabled bidirectional multilevel converter for solar PV powered electric vehicle charging," *Energy Reports*, 2025.

[13] S. Ramesh, M. Lingamaiah, and P. Ramesh, "Optimal control strategy for photovoltaic-battery powered electric vehicle using sliding mode control and linear quadratic regulator," *Scientific Reports*, 2025.

[14] J. O'Donovan, M. Hayes, and P. McCarthy, "Sliding mode control for bidirectional DC–DC power converter in electric vehicle charger for grid-to-vehicle and vehicle-to-grid applications," *IEEE Access*, 2025.

[15] R. Singh and V. Agarwal, "Design and control of bidirectional DC–DC converter for electric vehicle fast charging application," *IEEE Transactions on Transportation Electrification*, 2024.

[16] L. Zhao, Y. Zhang, and H. Li, "Modeling and small-signal analysis of bidirectional DC–DC converter for energy management in electric vehicle battery systems," *IEEE Access*, 2023.

[17] A. T. Rahman, M. S. Hossain, and K. M. Muttaqi, "A high-efficiency bidirectional isolated DC–DC converter with soft-switching for photovoltaic and battery interfacing," *IEEE Journal of Emerging and Selected Topics in Power Electronics*, 2024.

[18] S. K. Singh, D. P. Kothari, and M. J. Kumar, "Review of control techniques for bidirectional DC–DC converters in electric vehicle and renewable integration," *Renewable and Sustainable Energy Reviews*, 2025.

[19] J. Wang, C. Wang, and Z. Qian, "PID and fuzzy logic based hybrid control strategy for bidirectional DC–DC converters in microgrid energy systems," *Electric Power Systems Research*, 2023.

[20] N. S. Choudhary and P. S. Bimbhra, "Sliding mode control design of bidirectional DC–DC converter with constant power load for electric vehicle charging," *International Journal of Power Electronics and Drive Systems*, 2022.